

Design of terahertz varifocal devices based on dielectric metasurface

Mingxuan Tan

Key laboratory of Specialty Fiber Optics and Optical Access Networks,
Shanghai University, China, 200444

ABSTRACT

This paper presents the design of a rotational varifocal metasurface lens based on the principle of moiré lenses, utilizing square single-crystal silicon pillars. The metalens comprises two cascaded face-to-face metasurfaces, enabling focal length adjustment through the mutual rotation of these two metasurfaces. This design achieves high transmittance and complete 2π phase coverage. And through simulation verification, by rotating one layer of the metasurface from 60° , 72° , 90° , and 120° , the focal length of the designed moiré metalens shifts from 5.68 mm to 2.39 mm along the $-z$ direction on the xz plane, proving that the focus-shifted metalens we designed can be controlled by independently rotating the single-layer metasurface to adjust the focal length within the same focal plane.

Keywords: Dielectric metasurface, metalens, varifocal

1. INTRODUCTION

The metasurface is composed of ultra-thin two-dimensional structures, containing optical micro-antennas made of metal or dielectric for wavefront modulation. It has gained significant attention in recent years, with extensive research into its applications. As individual antennas influence the amplitude, phase, and polarization of transmitted or reflected waves, they depend on antenna dimensions, shapes, materials, spacing, and surrounding medium [1-2]. Consequently, metasurface-based devices like holograms, deflectors, and waveplates have been developed. Metasurfaces offer advantages such as small volume, easy integration into semiconductor devices, and high design flexibility, addressing issues like chromatic aberration and monochromatic aberration in traditional optical components. Recent studies indicate that a single or double-layer metasurface can resolve aberration problems that traditionally required multiple lenses in a system, significantly enhancing the compactness of optical systems [3-5].

Traditional geometric optical systems adjust focal length by moving lens groups, which increases the overall system size. Finding a way to achieve adjustable focus without enlarging the size became a concern [6]. Moiré lenses offer a solution, composed of two parallel phase plates based on diffractive optical elements. The phase distribution across the entire lens depends on the combination of these two plates [7]. As the plates rotate relative to each other, the lens's focal length changes accordingly. Therefore, by rotating these plates, the focal length of the lens can be adjusted. Compared to traditional focusing mechanisms, moiré lenses have the advantage of being compact and offering a wider range of focus adjustment [8]. With the development of diffractive optical elements [9-10], moiré superlenses have been demonstrated to be feasible at microwave, infrared a and infrared b wavelengths.

In this paper, we propose a polarization-independent variable-focus metalens. The simulation results show that by rotating one of the metasurfaces from 60° to 120° , the focal length of the designed moiré metalens can be adjusted from 5.68 mm to 2.39 mm along the $-z$ direction on the xz plane, realizing the focal length adjustment function. These components possess simple structures and are easily integrable, enhancing their practical utility in real-world applications.

2. DESIGN PRINCIPLES

This section first introduces the generalized Snell's law, and based on the derivation of the formula, constructs the phase distribution diagram of the moiré superlens at different angles when the rotation angle θ between the two metasurfaces is different. Finally, the artificial atom design method of the superlens is introduced.

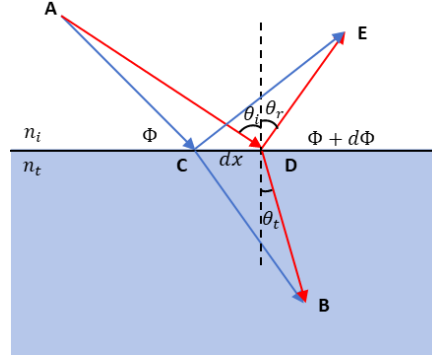


Figure 1. The generalized Snell's law.

Figure 1 is a schematic diagram of the generalized Snell's law, where Φ is the sudden phase of the interface between two media, n_i and n_t are the refractive indices of the two interface media, θ_t is the angle between the refracted light and the normal, and θ_i is the angle between the incident light and the normal. According to the Fermat principle, we can get:

$$[k_0 n_i \sin(\theta_i) dx + \Phi + d\Phi] - [k_0 n_t \sin(\theta_t) dx + \Phi] = 0 \quad (1)$$

Where the wave vector $k_0 = 2\pi/\lambda_0$ is the number of wavelengths in one spatial length, Φ and $\Phi + d\Phi$ are the phase changes, and a phase mutation Φ is introduced on the interface. The phase mutation amount is a function of the position coordinates on the interface, which is manifested as a non-fixed phase change. Since the two light paths achieve the effect of real light paths, dx can be regarded as infinitely small. If the phase changes of two adjacent points on the metasurface are consistent, the phase change between them is stable, thereby achieving the beam deflection effect. Then it can be deduced from the above formula

$$\sin(\theta_t) n_t - \sin(\theta_i) n_i = \frac{\lambda_0}{2\pi} \frac{d\Phi}{dx} \quad (2)$$

Where dx and $d\Phi$ are the distance and phase difference between the two optical paths at the interface, respectively. $d\Phi/dx$ is the phase gradient along the horizontal direction on the interface, which can be regarded as an additional phase gradient on the interface.

In the design of metasurface-based lenses, in order to focus the plane waves reaching the metasurface to the same focal point and achieve a focusing effect, the phase of the metasurface should meet specific conditions:

$$\Phi(r) = \frac{2\pi}{\lambda} (\sqrt{f^2 + r^2} - f) \approx \frac{\pi r^2}{\lambda f} \quad (3)$$

In the equation, $r = \sqrt{x^2 + y^2}$ is the radial coordinate of the metasurface, and f is the focal length, which represents the position of the focus. This formula shows that by introducing a suitable phase gradient along the interface direction through the metasurface, the refracted light beam can have an "arbitrary" direction.

The moire metalens is composed of two layers of metasurfaces cascaded. By independently rotating the two metasurfaces, the total phase distribution of the entire metalens can be dynamically changed, thereby achieving dynamic control of the focus position over a wide range, ranging from negative to positive values. The phase profiles of the two metasurfaces are Φ_{first} and Φ_{second} , respectively, in polar coordinates, (r, φ) can be expressed as

$$\begin{aligned} \Phi_{first}(r, \varphi) &= \text{round}(\alpha r^2 \varphi) \\ \Phi_{second}(r, \varphi) &= -\text{round}(\alpha r^2 \varphi) \end{aligned} \quad (4)$$

Where α is a constant. Formula (4) shows that the second metasurface has a phase profile that is upside down with the first metasurface. When one metasurface is rotated by an angle θ relative to the other metasurface, the phase profile $\Phi_{moire}(\theta)$ of the moire metalens is:

$$\Phi_{moire} = \Phi_{first}(r, \varphi) + \Phi_{second}(r, \varphi - \theta) = \text{round}(\alpha r^2 \theta) \quad (5)$$

Comparing formula (3) with formula (5), it is easy to see that we can adjust the position of the moire metalens focal point by changing the angle θ between the first metasurface and the second metasurface

$$f^{-1}(\theta) = \frac{\alpha\lambda\theta}{\pi} \quad (6)$$

According to the above formula, the gradient phase distribution of the two layers of metasurfaces along the z direction is set to $\Phi = k_0 \sin(\theta)z$, where θ is the rotation angle between the two layers of metasurfaces. Figure 2 below shows the phase distribution of the moire metalens when the rotation angle θ between the two layers of metasurfaces is 60°, 72°, 90°, 120° respectively.

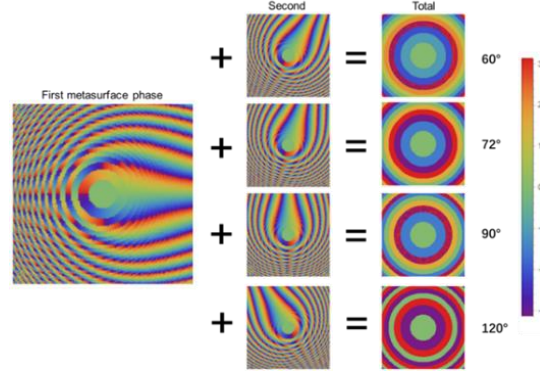


Figure 2. The Phase distribution diagram of each layer of the metasurface and the overall metalens at different mutual rotation angles

The following will introduce the design of artificial atoms that constitute cascade superlenses, in which the material selection of artificial atoms is a key issue in dielectric superlenses. Waveguide-type artificial atoms working in the visible light band usually use materials with wide band gaps, including titanium oxide, silicon nitride, and gallium nitride. However, the increase in the band gap often corresponds to a decrease in the refractive index, which requires an increase in the aspect ratio and sacrifices efficiency to achieve 2π phase coverage. Studies have shown that silicon is an indirect semiconductor, which has the characteristic that its extinction coefficient will not increase significantly in the wavelength range exceeding the band gap.

Therefore, in order to ensure that the designed superlens has high transparency, based on the excellent properties of silicon, this paper selects a group of all-dielectric artificial atoms with high transmission efficiency for 0.6 THz waves. The artificial atom adopts the unit structure shown in Figure 3(a) and completes the focus shift through the resonant phase to realize the function of the moire superlens. The structure consists of three layers, in which the middle layer is a silicon dielectric layer ($\epsilon_{si} = 11.6$), and the upper and lower layers are composed of two silicon pillars with square cross-sections, which are deposited on different surfaces of the continuous silicon partition. The silicon pillar at the bottom is mainly used to reduce the reflection of the artificial atom to the terahertz wave, while the top part realizes the accumulation of the transmission phase by changing the cross-sectional side length (w). Therefore, we need to optimize the cross-sectional side length (w) of the top silicon pillar to ensure that the artificial atom can produce the required phase shift.

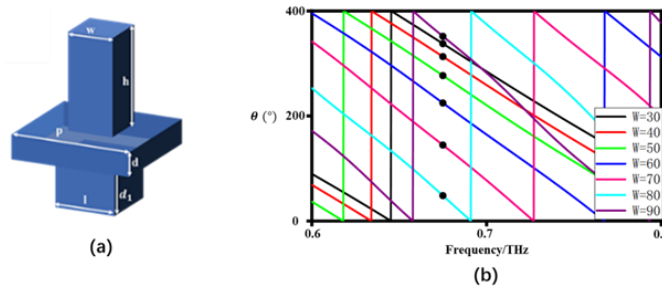


Figure 3. (a) the component structure and geometric parameters. (b) the distribution of phase differences as w varies

The side length of the upper square silicon column is w , and the height is h . The side length of the lower square silicon column is l , and the height is d_1 . The period of the middle silicon dielectric layer in the xy plane is p , and the thickness is d . The specific parameters of the three-layer structure are: $l = 74\mu\text{m}$, $d = 44\mu\text{m}$, $p = 110\mu\text{m}$, $d_1 = 111\mu\text{m}$, $h = 310\mu\text{m}$.

After we determine the parameters of the artificial atoms, we can obtain the corresponding transmission phase by changing w , so as to establish an artificial atom library to quickly select suitable artificial atoms and produce different phase mutations at different positions of the metasurface. Figure 3 (b) shows that by changing the side length w of the upper square silicon dielectric column from $30\mu\text{m}$ to $90\mu\text{m}$, we can achieve a $0-2\pi$ phase shift, which helps us to realize the function of controlling the focus position.

3. NUMERICAL SIMULATION AND RESULTS

In this part, based on the previous theoretical preparation and artificial atom library, a focus-shifted superlens was designed based on the artificial atom in Figure 3 (a) and its function was preliminarily verified using CST simulation software. In Figure 4, the metasurface is simulated in a circular shape to facilitate rotation. The diameter of the metasurface is 3.92 mm , and the distance between the two layers of the metasurface is selected to be $300\text{ }\mu\text{m}$ to eliminate the diffraction effect and ensure the stability of the entire system.

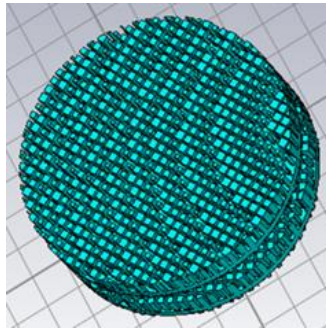


Figure 4. Cascaded Metasurfaces, composed of two layers of rotatable circular metasurfaces

After the simulation conditions are set, a full-wave simulation is performed on the metalens. As shown in Figure 5, the focus formed at different rotation angle differences ($\theta = 60^\circ, 72^\circ, 90^\circ, 120^\circ$) between the two metasurfaces at a frequency of 0.6 THz is obtained (the position of the focus is defined as the point where the normalized electric field intensity is the maximum). Figures 5(a)-5(d) respectively show the electric field intensity distribution of the focus in the xz plane under different rotation angle differences. When $\theta = 60^\circ$, we can clearly see that the lateral position of the focus is at $(0, 5.68)$. As the rotation angle difference θ between the two metasurfaces increases, the focus gradually shifts along the $-z$ direction. When θ increases to 120° , a well-focused light spot can still be found. Figures 5(e)-5(h) show the normalized electric field intensity distribution and the corresponding lateral intensity distribution of the focal plane in the xy plane.

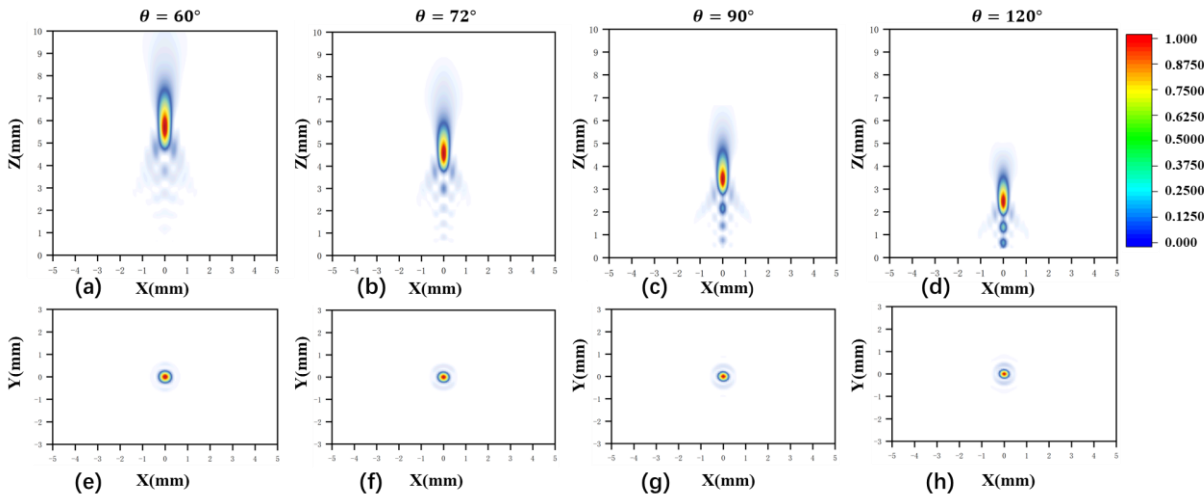


Figure 5. The figure displays the focal electric field distribution of the metalens at different rotation angles ($\theta = 60^\circ, 72^\circ, 90^\circ, 120^\circ$), corresponding to the field distributions in the xz plane (a)-(d). The focal plane field distributions (e)-(h) correspond respectively to the xy plane field distributions at rotation angles of $\theta = 60^\circ, 72^\circ, 90^\circ, 120^\circ$

Obviously, the full-wave simulation results can prove that the focus-shifted metalens we designed can control the focus to zoom in the same focal plane by independently rotating the single-layer metasurface.

4. CONCLUSION

This paper proposes an all-dielectric metasurface composed of silicon pillar arrays of different sizes. On this basis, a variable-focus superlens consisting of two cascaded supersurfaces is designed. Under normal incident polarized light, the phase coverage range is from 0 to 2π . The simulation results show that the focal length of the designed moiré superlens shifts from 5.68 mm to 2.39 mm along the -z direction on the xz plane, proving that the focus-shifted superlens designed by us can adjust the focal length in the same focal plane by independently rotating the single-layer metasurface. At the same time, compared with traditional terahertz devices, the superlens designed based on the metasurface has a simple structure and is easy to manufacture. In the future, by carefully designing each single-layer metasurface, other components with different wave manipulation functions can also be realized. The current drawback is that the design has not been experimentally verified.

REFERENCES

- [1] R. Izumi, S. Ikezawa, and K. Iwami, "Metasurface holographic movie: a cinematographic approach," *Opt. Express*, vol. 28, no. 16, pp. 23761–23770, 2020
- [2] E. Arbabi, A. Arbabi, S. M. Kamali, Y. Horie, M. S. Faraji-Dana, and A. Faraon, "MEMS-tunable dielectric metasurface lens" *Nat. Commun.*, vol. 9, no. 1, p. 812, 2018
- [3] W. T. Chen, A. Y. Zhu, V. Sanjeev, et al., "A broadband achromatic metalens for focusing and imaging in the visible," *Nat. Nanotechnol.*, vol. 13, no. 3, pp. 220–226, 2018
- [4] W. T. Chen, A. Y. Zhu, J. Sisler, Z. Bharwani, and F. Capasso, "A broadband achromatic polarization-insensitive metalens consisting of anisotropic nanostructures," *Nat. Commun.*, vol. 10, no. 1, pp. 1–7, 2019.
- [5] D. Hakobyan, H. Magallanes, G. Seniutinas, S. Juodkazis, and E. Brasselet, "Tailoring orbital angular momentum of light in the visible domain with metallic metasurfaces," *Adv. Opt. Mater.*, vol. 4, no. 2, pp. 306–312, 2016
- [6] Kentaro Iwami, Chikara Ogawa, Tomoyasu Nagase, and Satoshi Ikezawa, "Demonstration of focal length tuning by rotational varifocal moiré metalens in an ir-A wavelength," *Opt. Express* 28, 35602-35614 (2020)
- [7] Guocui Wang, Tian Zhou, Jianzhou Huang, Xinke Wang, Bin Hu, and Yan Zhang, "Moiré meta-device for flexibly controlled Bessel beam generation," *Photon. Res.* 11, 100-108 (2023)
- [8] Jung, Joonkyo, Kim, Hyeonhee and Shin, Jonghwa. "Three-dimensionally reconfigurable focusing of laser by mechanically tunable metalens doublet with built-in holograms for alignment" *Nanophotonics*, vol. 12, no. 8, 2023, pp. 1373-1385.
- [9] S. Bernet and M. Ritsch-Marte, "Adjustable refractive power from diffractive moiré elements," *Appl. Opt.*, vol. 47, no. 21, pp. 3722–3730, 2008.
- [10] S. Bernet, W. Harm, and M. Ritsch-Marte, "Demonstration of focus-tunable diffractive Moiré lenses," *Opt. Express*, vol. 21, no. 6, pp. 6955–6966, 2013.